# Crystallization Behavior of Polyamide 11/Multiwalled Carbon Nanotube Composites

**Zhe Yang, Shu Huang, Tianxi Liu**

*Key Laboratory of Molecular Engineering of Polymers of Ministry of Education, Department of Macromolecular Science, Fudan University, Shanghai 200433, China*

Received 2 November 2010; accepted 4 January 2011
DOI 10.1002/app.34118
Published online 27 April 2011 in Wiley Online Library (wileyonlinelibrary.com).

**ABSTRACT:** Differential scanning calorimetry (DSC) was used to investigate the isothermal and nonisothermal crystallization kinetics of polyamide11 (PA11)/multiwalled carbon nanotube (MWNTs) composites. The Avrami equation was used for describing the isothermal crystallization behavior of neat PA11 and its nanocomposites. For nonisothermal studies, the Avrami model, the Ozawa model, and the method combining the Avrami and Ozawa theories were employed. It was found that the Avrami exponent $n$ decreased with the addition of MWNTs during the isothermal crystallization, indicating that the MWNTs accelerated the crystallization process as nucleating agent. The kinetic analysis of nonisothermal crystallization process showed that the presence of carbon nanotubes hindered the mobility of polymer chain segments and dominated the nonisothermal crystallization process. The MWNTs played two competing roles on the crystallization of PA11 nanocomposites: on the one hand, the MWNTs serve as heterogeneous nucleating agent promoting the crystallization process of PA11; on the other hand, the MWNTs hinder the mobility of the polymer chains thus retarding the crystal growth process of PA11. The activation energies of PA11/MWNTs composites for the isothermal and nonisothermal crystallization are lower than neat PA11.
 J Appl Polym Sci 122: 551–560, 2011

**Key words:** polyamide 11; carbon nanotubes; nanocomposites; crystallization

## INTRODUCTION

Carbon nanotubes are considered to be one kind of ideal one-dimensional reinforcing fillers for fabricating high-performance polymer composites because of their nanoscale diameter, high aspect ratio, and unique physical properties (such as excellent mechanical strength, thermal, and electrical conductivities).[1,2] Many researchers have fabricated various polymer/carbon nanotube nanocomposites with different excellent properties.[3,4] When carbon nanotubes are introduced to the semicrystalline polymers, this rigid filler will act as nucleating agent and induce polymer crystallization. For example, Assouline et al. investigated the nucleation ability of multiwalled carbon nanotubes (MWNTs) in polypropylene composites and found that the MWNTs accelerated the crystallization change by acting as α phase nucleating agent in isotactic PP.[5] Wu et al. reported that the addition of c-MWNTs (multiwalled carbon nanotubes containing carboxylic groups) into poly(ε-caprolactone) (PCL) induced the heterogeneous nucleation at low c-MWNT content and then inhibited the polymer chain transportation ability during crystallization at high c-MWNT content.[6,7] The nucleation effect of carbon nanotubes in polyamide 6 (PA6), PA66, poly(L-lactide), and poly(ethylene terephthalate) (PET) matrices was also studied.[8–11]

Polyamide 11 (PA11), a polymer which is widely used for industrial applications, possesses excellent piezoelectric behavior, plus good cryogenic, oil resistance, and water resistance properties, although its impact properties, tensile strength, and thermal properties are somewhat poor. It is well understood that the physical and mechanical properties of crystalline polymers greatly depend on the morphology, crystalline structure, and degree of crystallinity. To improve the mechanical properties of PA11, its nanocomposites with various MWNTs loadings have been successfully prepared by our group using a melt-compounding approach.[12] It was shown that the addition of MWNTs markedly improved the mechanical properties of PA11 composites. Zhou et al. prepared PA11/MWNTs by using *in situ* polymerization method.[13] Different kinds of fillers have different effects on crystallization behavior in polymer nanocomposites. Gunes et al. investigated the

*Correspondence to:* T. Liu (txliu@fudan.edu.cn).
Contract grant sponsor: National Natural Science Foundation of China; contract grant numbers: 20774019, 50873027.
Contract grant sponsor: Shanghai Municipal Education Commission and Shanghai Education Development Foundation ("Shu Guang" project); contract grant number: 09SG02.

influence of fillers on crystallization of shape memory polymers and illustrated that the effect of nanofillers on crystallization could not be considered as originating from physical presence only, and a decrease in crystallinity has been reported in polymer matrix caused by adding different nanofillers.[14–16] It is of great importance to investigate the critical effect of the MWNTs on PA11 crystallization. In this article, isothermal and nonisothermal experiments were conducted to study the crystallization behavior of PA11/MWNTs nanocomposites by using several kinetic methods.

## EXPERIMENTAL

### Materials and sample preparation

PA11 pellets used in this study were purchased from Atofina (Rilsan Besno TL, Atofina). Since polyamides are very easy to absorb moisture, before compounding all the samples were dried in vacuum oven at 80°C for 24 h to remove the absorbed water. The MWNTs were prepared by catalytic chemical vapor deposition of methane on Co-Mo/MgO catalysts, according to the procedures reported previously.[17] The catalyst in the as-prepared MWNTs sample was removed by dissolving in concentrated nitric acid (Shanghai Chemical Reagent Co., Shanghai, China), and then the MWNTs powder was filtered and washed with deionized water for at least five times. The MWNTs were further refluxed in 2.6*M* nitric acid to increase more carboxylic and hydroxyl groups on the surface of the MWNTs. A range of PA11/MWNTs nanocomposites containing 0, 0.2, 0.5, and 1.0 wt % MWNTs was prepared via melt compounding using a Brabender twin-screw extruder at 220°C with a screw speed of 80 rpm.

### Characterization

Isothermal and nonisothermal crystallization kinetics was performed using a Pyris 1 differential scanning calorimeter (DSC) (Perkin–Elmer, Norwalk, CT). The instrument was calibrated with high-purity indium and zinc. For melt crystallization, the samples were heated up to 230°C and held there for 5 min to remove small nuclei that might act as seeding crystals. Isothermal crystallization experiments were performed as follows: the sample was heated to 230°C at a rate of 20°C/min and held there for 5 min to eliminate any previous thermal history, and then cooled at a rate of −50°C/min to the predetermined crystallization temperature ($T_c$), ranged from 160 to 182°C with a step of 2°C. The sample was maintained at $T_c$ for 1 h to get the DSC trace returned to the calorimeter baseline. For nonisothermal crystallization process, the samples were crystallized at different cooling rates of 2.5, 5, 10, 15, and 20°C/min. All the experiments were carried out in sealed pans under dry nitrogen environment.

## RESULTS AND DISCUSSION

### Isothermal crystallization kinetics

The effect of MWNTs on the crystallization behavior of PA11 can be analyzed using the Avrami equation.[18,19] The relative crystallinity, $X(t)$, at time $t$, is defined as follows:

$$X(t) = X_c(t)/X_c(t_\infty) = \int_0^t \frac{dH_c}{dt}dt \Big/ \int_0^{t_\infty} \frac{dH_c}{dt}dt \quad (1)$$

The Avrami equation is given as follows:

$$1 - X_t = \exp(-Z_t t^n) \quad (2a)$$

or

$$\log\{-\ln[1 - X(t)]\} = n \log t + \log Z_t \quad (2b)$$

where $n$ is a constant that depends on both the nucleation and growth of the crystals, and $Z_t$ is the crystallization rate constant. Figure 1(a,b) show the relationship between $X(t)$ and $t$, and plots of $\log\{-\ln [1 - X(t)]\}$ versus $\log(t)$ during isothermal crystallization for neat PA11 and PA11/MWNTs (99.8/0.2) nanocomposite. It can be seen that all curves are fitted well with the Avrami equation and result in linear relationships, indicating that the Avrami method is suitable for describing the isothermal crystallization behavior of PA11 and PA11/MWNTs nanocomposites. Using the plots of $\log\{-\ln [1 - X(t)]\}$ versus $\log(t)$, the values of $n$ and $Z_t$ can be obtained from the slope and intercept, respectively, as listed in Table I. It can be concluded that the value of $n$ varies from 1.7 to 2.4, depending on the loading level of MWNTs and the crystallization temperature. Thus, it may be inferred that the crystal growth of PA11 nanocomposites does not completely follow the three-dimensional spherulitic propagation. We can also see that the value of $n$ decreases after adding MWNTs into PA11 matrix, indicating that the MWNTs act as nucleating agent and thus result in a change in the nucleation mechanism of PA11. The following two factors may be the reasons leading to the decrease of $n$ value[9,20]: (1) MWNTs act as 1D nuclei in the PA11 matrix; (2) The carboxylic and hydroxyl groups of the nanotubes induce dense nucleation on the surfaces of the MWNTs. Therefore, the crystal growth for PA11 chains is confined within the adjacent crystals and the dimension is thus decreased.

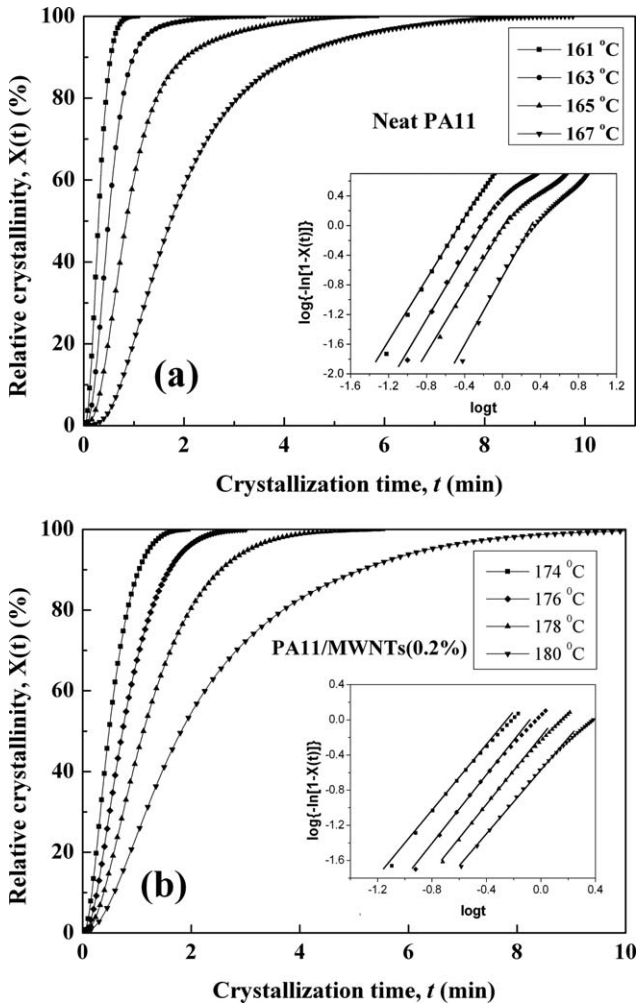


**Figure 1** Relative crystallinity, $X(t)$, at different crystallization times, $t$, and plots of $\log\{-\ln[1 - X(t)]\}$ as a function of $\log(t)$ during the process of isothermal crystallization for (a) neat PA11 and (b) PA11/MWNTs (99.8/0.2) nanocomposite.

The crystallization half-time, $t_{1/2}$, is defined as the time at which the extent of crystallization is 50% complete and is determined from the measured kinetic parameters as follows:

$$t_{1/2} = (\ln 2/Z_t)^{1/n} \tag{3}$$

The maximum crystallization, $t_{max}$, is defined as follows:

$$t_{max} = [(n-1)/nZ_t]^{1/n} \tag{4}$$

Table I also presents the values of $t_{1/2}$ and $t_{max}$. As nucleating agent, the MWNTs significantly increase the temperature of melt crystallization for PA11. Therefore, it is difficult to compare isothermal crystallization rates of neat PA11 with those of PA11/MWNT composites at the same crystallization temperature. However, the $t_{1/2}$ decreases with increasing the MWNTs content in the nanocomposites, indicating that the MWNTs can accelerate polymer crystallization.

The crystallization process for bulk PA11 is assumed to be thermally activated, and then the crystallization rate parameter $Z_t$ can be approximately described by the following Arrhenius relationship[21]:

$$Z_t^{1/n} = k_0 \exp(-E/RT_c) \tag{5a}$$

or

$$\frac{1}{n}\ln Z_t = \ln k_0 - \frac{\Delta E}{RT_c} \tag{5b}$$

where $k_0$ is a temperature-independent pre-exponential factor, $R$ is the gas constant, and $\Delta E$ is the crystallization activation energy. $\Delta E$ can be determined by the slope coefficients of plots of $(1/n)\ln(Z_t)$ as a function of $1/T_c$ (Fig. 2). Figure 3 shows the effect of the MWNT content on the $\Delta E$ of isothermal crystallization for PA11. It can be seen that the crystallization activation energy of PA11/MWNT composites is lower than that of neat PA11, whereas that of the composite containing 0.5 wt % MWNTs is the lowest and then increases with increasing the MWNTs content. This is probably because the crystallization of PA11 consists of both nucleation and crystal growth processes. When the MWNTs content is low (e.g., below 0.5 wt %), the strong nucleation effect of the nanotubes plays an important role in the PA11 nanocomposites, crystallization activation energy thus decreases compared with neat PA11. When the MWNTs loading level is high (e.g., 1.0 wt %), the

**TABLE I**
**Avrami Kinetic Parameters from the Avrami Equation for the Isothermal Crystallization of Neat PA11 and Its MWNTs Nanocomposites**

| | $T_c$ (°C) | $n$ | $K$ | $t_{1/2}$ (min) | $t_{max}$ (min) |
|---|---|---|---|---|---|
| Neat PA11 | 161 | 2.1 | 9.14 | 0.300 | 0.266 |
| | 163 | 2.2 | 2.99 | 0.513 | 0.459 |
| | 165 | 2.2 | 0.97 | 0.859 | 0.769 |
| | 167 | 2.4 | 0.20 | 1.700 | 1.577 |
| PA11/MWNTs (0.2%) | 174 | 1.8 | 2.54 | 0.488 | 0.383 |
| | 176 | 1.8 | 1.21 | 0.740 | 0.588 |
| | 178 | 1.8 | 0.56 | 1.131 | 0.872 |
| | 180 | 1.7 | 0.26 | 1.807 | 1.315 |
| PA11/MWNTs (0.5%) | 176 | 1.9 | 2.24 | 0.540 | 0.442 |
| | 178 | 1.8 | 0.90 | 0.866 | 0.693 |
| | 180 | 1.9 | 0.51 | 1.181 | 0.954 |
| | 182 | 1.7 | 0.33 | 1.525 | 1.144 |
| PA11/MWNTs (1.0%) | 176 | 1.8 | 4.62 | 0.343 | 0.265 |
| | 178 | 1.8 | 2.48 | 0.493 | 0.384 |
| | 180 | 1.8 | 1.77 | 0.588 | 0.452 |
| | 182 | 1.8 | 0.48 | 1.243 | 0.953 |

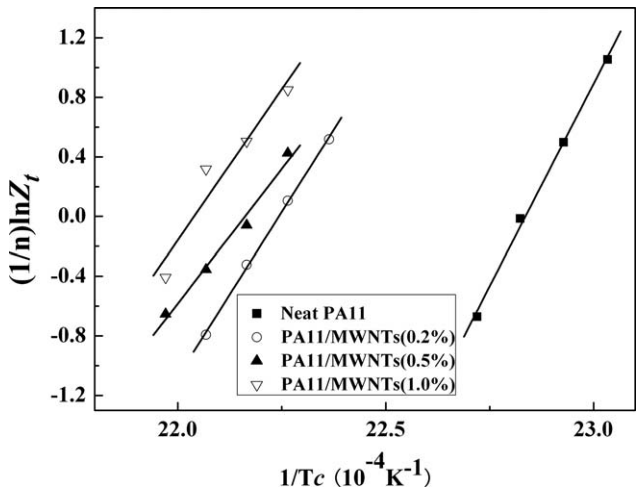


**Figure 2** Plots of $(1/n)\ln(Z_t)$ versus as a function of $1/T_c$ for the Avrami parameter $Z_t$ from the isothermal crystallization process.

presence of more nanotubes would result in much more steric hindrance thus reducing the transportation ability of polymer chains during crystallization. It should be noted that the surface property of MWNTs may have a great influence on the crystallization of the matrix polymer. Deng et al. found that the functional groups on the MWNTs surface influenced the thermal and mechanical property of PA6 matrix, which is caused by the reduced chain mobility in the system because of the interactions between functional groups.[22] Therefore, the crystallization activation energy increases when further increasing the content of MWNTs. These nanoscale confinement and multiple nucleation effects of the MWNTs were also found in PCL/MWNTs and PA6/MWNTs nanocomposites.[6,8]

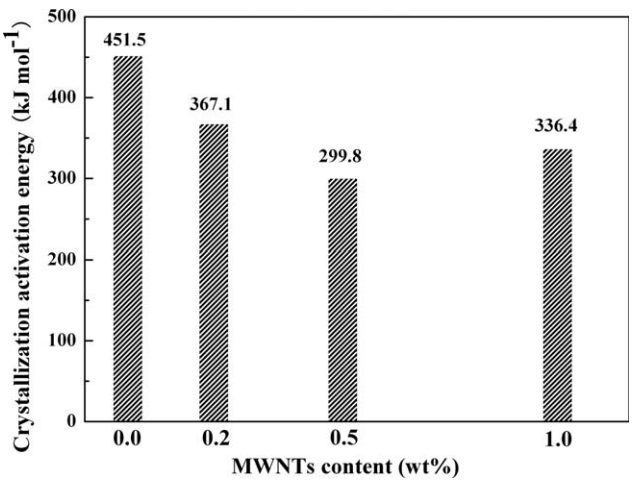


**Figure 3** Effect of MWNTs on the isothermal crystallization activation energy of PA11.

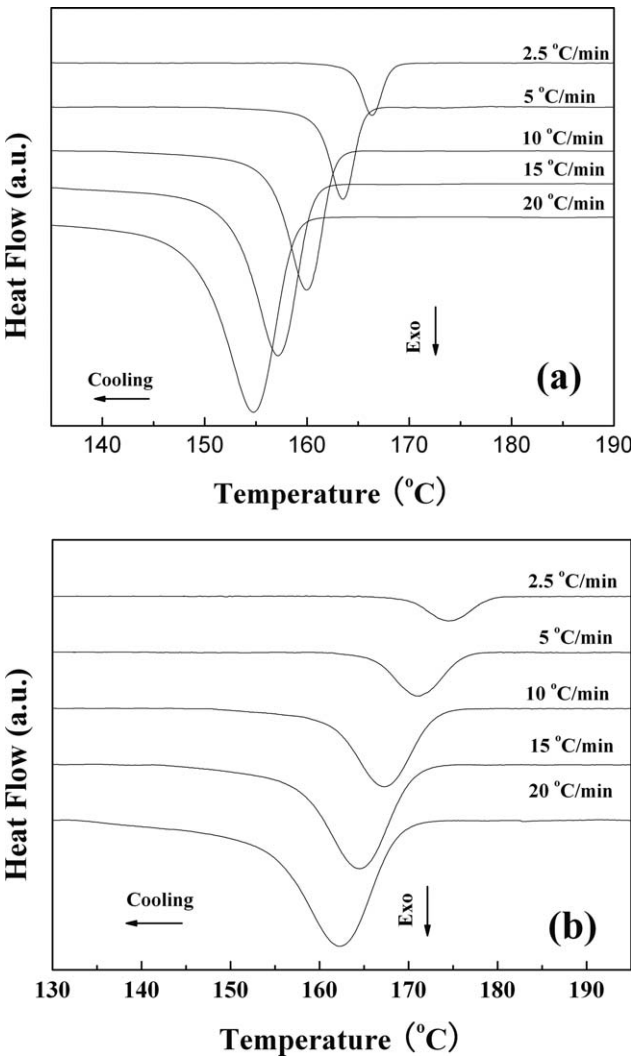


**Figure 4** DSC curve of nonisothermal melt crystallization for (a) neat PA11 and (b) PA11/MWNTs (99.8/0.2) nanocomposite.

### Nonisothermal crystallization kinetics

The crystallization exotherms of PA11 and its composites at various cooling rates are illustrated in Figure 4. The nonisothermal crystallization peak temperature, $T_p$, peak time, $t_{Tp}$, and the crystallization enthalpies, $\Delta H_c$, at different cooling rates obtained from Figure 4 are summarized in Table II. For both neat PA11 and its composites, as the cooling rate increases, the crystallization peak becomes broader and the $T_p$ shifts to lower temperature, indicating that the lower the cooling rate is, the earlier the crystallization occurs. When the samples were cooled quickly from the melt, the motion of the polymer chains could not follow the cooling rate. Therefore, more supercooling was required to initiate crystallization at higher cooling rate.[23–25] It can be concluded from Table II that, at a given cooling rate, the $T_p$ values of PA11/MWNTs composites were slightly higher than that of neat PA11. This can

**TABLE II**
**Peak Temperature ($T_p$), Time ($t_{Tp}$), Crystallization Enthalpy ($\Delta H_c$), and Relative Crystallinity ($X_t$) at Maximum Rate of Heat Flow and Half-Time of Crystallization ($t_{1/2}$) During Nonisothermal Melt Crystallization of PA 11 and PA11/MWNTs Composites**

| | $\Phi$ (°C/min) | $T_p$ (°C) | $t_{Tp}$ (min) | $\Delta H_c$ (J/g) | $X_{t,Tp}$ (%) | $t_{1/2}$ (min) |
|---|---|---|---|---|---|---|
| Neat PA11 | 2.5 | 166 | 1.0 | 42.1 | 43 | 1.1 |
| | 5 | 164 | 0.6 | 48.0 | 40 | 0.7 |
| | 10 | 160 | 0.5 | 49.9 | 36 | 0.6 |
| | 15 | 157 | 0.4 | 54.0 | 34 | 0.4 |
| | 20 | 155 | 0.3 | 56.4 | 31 | 0.4 |
| PA11/MWNTs (0.2%) | 2.5 | 175 | 2.8 | 33.6 | 48 | 2.8 |
| | 5 | 171 | 1.6 | 36.0 | 46 | 1.7 |
| | 10 | 167 | 0.9 | 36.6 | 43 | 0.9 |
| | 15 | 165 | 0.7 | 38.5 | 41 | 0.7 |
| | 20 | 162 | 0.5 | 40.6 | 38 | 0.5 |
| PA11/MWNTs (0.5%) | 2.5 | 176 | 3.1 | 35.5 | 42 | 3.4 |
| | 5 | 172 | 2.3 | 36.5 | 41 | 2.3 |
| | 10 | 168 | 0.7 | 39.0 | 43 | 0.8 |
| | 15 | 165 | 0.5 | 40.2 | 39 | 0.6 |
| | 20 | 163 | 0.5 | 40.8 | 37 | 0.5 |
| PA11/MWNTs (1.0%) | 2.5 | 176 | 2.7 | 40.3 | 40 | 2.9 |
| | 5 | 173 | 1.7 | 40.4 | 40 | 1.8 |
| | 10 | 169 | 0.7 | 43.0 | 43 | 0.8 |
| | 15 | 166 | 0.6 | 43.6 | 41 | 0.6 |
| | 20 | 163 | 0.5 | 46.1 | 41 | 0.6 |

be explained by the theory proposed by Ebengou.[26] The MWNTs had a heterogeneous nucleation effect on the polymer chains, which could be easily attached to the surfaces of the MWNTs. As a result, the crystallization of PA11 was promoted and occurred at a higher crystallization temperature.

To further analyze the nonisothermal crystallization process, the crystallization kinetics of neat PA11 and PA11/MWNTs nanocomposites is compared. The relative crystallization of nonisothermal crystallization, which is defined as a function of temperature, can be expressed as eq. (6):

$$X_t = \int_{T_0}^{T} \left(\frac{dH_c}{dT}\right) dT \Big/ \int_{T_0}^{T_\infty} \left(\frac{dH_c}{dT}\right) dT \qquad (6)$$

where $T_0$ and $T_\infty$ represent the onset and end temperatures of crystallization, respectively, and $dH_c/dT$ is the heat flow rate. The development of $X_t$ with crystallization temperature at various cooling rates is presented in Figure 5.

During the nonisothermal melt crystallization process, the relationship between the crystallization time $t$ and the crystallization temperature $T$ can be described as follows:

$$t = (T_0 - T)/\Phi \qquad (7)$$

where $T$ is the temperature at crystallization time $t$, $T_0$ is the onset temperature of crystallization, and $\Phi$ is the cooling rate. According to eq. (7), the value of $T$ on the $X$-axis in Figure 6 can be transposed into the crystallization time $t$, as shown in Figure 6. The relative crystallinity $X_{t,Tp}$, and the crystallization time $t_{Tp}$ at different cooling rates are shown in Table II. The value of $X_{t,Tp}$ changes randomly between 30 and 50%. As the cooling rate became faster, $t_{Tp}$ became shorter. This indicates that the crystallization of neat PA11 and PA11/MWNTs nanocomposites occurred at higher temperature and took more time as the cooling rate decreased, implying that the crystallization is controlled by the nucleation process.[25]

The half crystallization time of nonisothermal crystallization ($t_{1/2}$) is defined as the time taken from the onset of crystallization to the time when $X_t$ is 50%. $t_{1/2}$ is defined as follows:

$$t_{1/2} = \frac{T_0 - T_{1/2}}{\Phi} \qquad (8)$$

where $T_{1/2}$ is the crystallization temperature corresponding to the relative crystallinity of 50%. The values of $t_{1/2}$ for neat PA11 and PA11/MWNTs nanocomposites are also listed in Table II. It can be seen that $t_{1/2}$ became lower as the cooling rate increased, also indicating that neat PA11 and its MWNTs nanocomposites crystallized faster when the cooling rate became higher. In addition, the $t_{1/2}$ values of PA11/MWNTs nanocomposites are higher than that of neat PA11, implying that the crystallization rate decreases when adding MWNTs into PA11 matrix. It seems that the MWNTs act as physical hindrance and thus retard the crystallization of PA11 in the nonisothermal crystallization process. This may be attributed to the higher interfacial area and interaction between PA11 chains and the

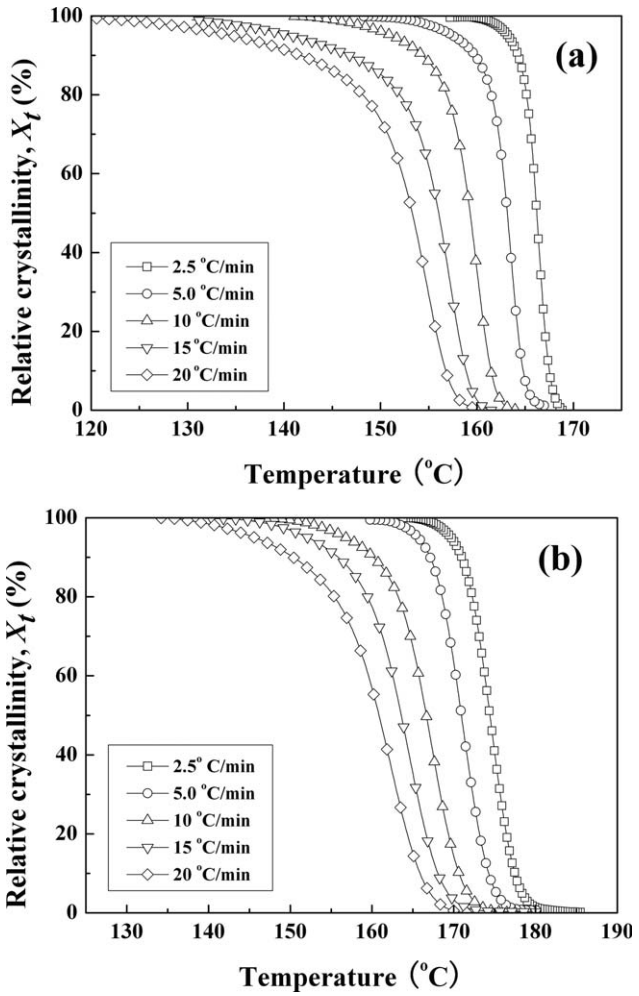


**Figure 5** Relative crystallinity, $X(t)$, at different crystallization temperatures, $T$, during the process of nonisothermal crystallization for: (a) neat PA11 and (b) PA11/MWNTs (99.8/0.2) nanocomposite.

surface-modified MWNTs, which can reduce the mobility of the polymer chains for crystallization. It can be concluded that the roles of the MWNTs are twofold: on one hand, the MWNTs act as heterogeneous nucleation agent in PA11 matrix; on the other hand, the interaction between the MWNTs and PA11 and the physical hindrance effect retard the crystallization of polymer chains. In previous studies on PA11/ZnO and PA6/montmorillonite composites, same changing trend of $t_{1/2}$ has been observed.[27–29]

To get a deep understanding of the nonisothermal crystallization process, the Avrami, the Ozawa, and the combined Avrami–Ozawa methods are used here to analyze the nonisothermal crystallization kinetics of PA11 and PA11/MWNTs nanocomposites. For nonisothermal crystallization, the parameters $n$ and $Z_t$ in the Avrami equation [eq. (2a) and (2b)] have an explicit physical meaning as in isothermal crystallization, due to the constant change in temperature. Although the physical meaning of $n$ and $Z_t$ cannot be related in a simple way to the isothermal case, the direct application of eq. (2a) and (2b) could still provide some insights in describing the nonisothermal crystallization kinetics of many polymeric systems.[30,31] Considering the nonisothermal character of the crystallization process investigated, Jeziorny pointed out that the value of rate parameter $Z_t$ should be adequately corrected.[32] The factor that should be considered was the cooling rate, $\Phi$. Assuming a constant or approximately constant value of $\Phi$, the final form of the parameter characterizing the kinetics of nonisothermal crystallization was given as follows:

$$\log Z_c = \frac{\log Z_t}{\Phi} \tag{9}$$

The values of the Avrami exponent $n$ and the rate parameter $Z_c$ can be determined from the slope and intercept of the plot of $\log[-\ln(1 - X_t)]$ versus $\log(t)$, respectively. The plots of $\log[-\ln(1 - X_t)]$ versus $\log(t)$ for PA11 and its MWNTs composites are shown in Figure 6. The Avrami exponent $n$, shown in Table III, is about 3, implying that the modes of the nucleation and the growth of both PA11 and PA11/MWNTs composites are complicated and the nucleation mode should be homogeneous thermal nucleation, and its crystal growth is three-dimensional spherulitic growth. We can see that for all the samples, the values of $n$ in nonisothermal crystallization become higher than those in isothermal crystallization. As reported previously,[33] the mode of spherulitic nucleation and growth for nonisothermal crystallization of PA11 is more complicated than that for isothermal crystallization process. In addition, the values of $Z_c$, listed in Table III, increase with increasing the cooling rate. The larger the rate parameter $Z_c$ value, the higher the crystallization rate is. Under the same cooling rate, higher $Z_c$ is obtained for PA11 than those for PA11/MWNTs composites, indicating that the presence of MWNTs hinders the growth of PA6 crystallite under nonisothermal condition, which is in accordance with the results of $t_{1/2}$.

Considering the nonisothermal crystallization being a rate dependent process, Ozawa extended the Avrami equation to the nonisothermal condition by replacing time variable in Avrami equation with a variable cooling rate and derived a kinetic equation as follows[34,35]:

$$1 - X_t = \exp\left[-\frac{K(T)}{\Phi^m}\right] \tag{10}$$

where $K(T)$ was a cooling function, and $m$ was Ozawa exponent depending on the crystal growth

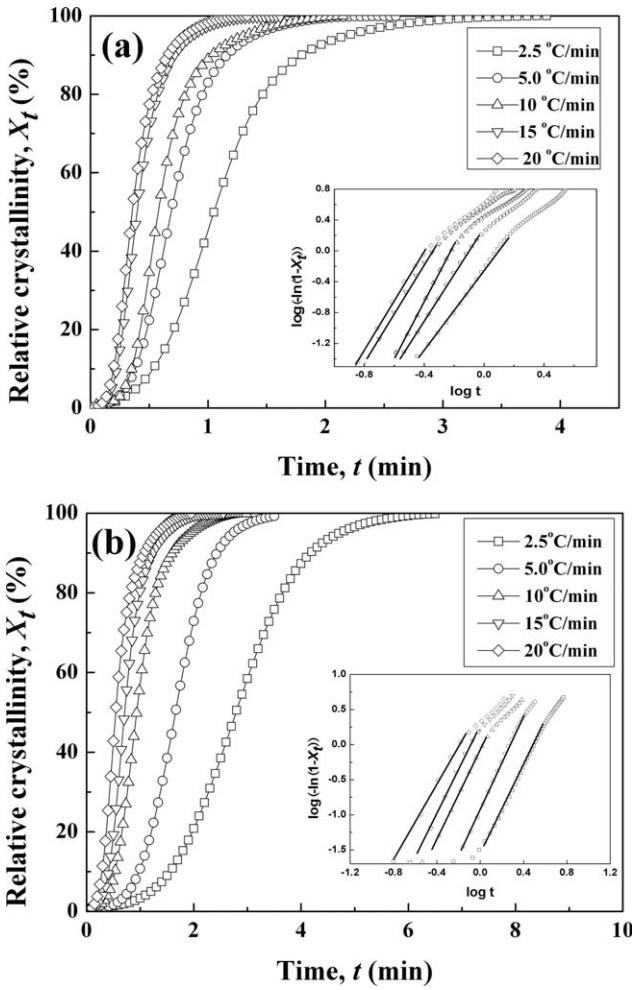


**Figure 6** Relative crystallinity, $X(t)$, at different crystallization times, $t$, during the process of nonisothermal crystallization for: (a) neat PA11 and (b) PA11/MWNTs (99.8/0.2) nanocomposite.

and nucleation mechanism. According to the double logarithmic form of eq. (10), the Ozawa plots of $\log[-\ln(1 - X_t)]$ versus $\log(\Phi)$ for PA11 and its MWNTs composites were shown in Figure 7. The $X_t$ values calculated at different temperatures decreased with increasing cooling rate at a given temperature. The continuous change in the slope of the plots clearly indicates that $m$ is not constant with temperature, and the cooling function $K(T)$ cannot be determined due to the curvature in the curves. The zig–zag lines in Figure 8 made it difficult to estimate the Ozawa exponent $m$ and the cooling function $K(T)$, indicating that the Ozawa analysis could not adequately describe the nonisothermal crystallization kinetics of neat PA11 and its composites. The reason may be due to the inaccurate assumption in Ozawa theory since nonisothermal crystallization is a dynamic process in which the crystallization rate is no longer constant but a function of time and cooling rate.

**TABLE III**
**Effect of Cooling Rate on the Nonisothermal Crystallization Kinetic Parameters of PA11 and PA11/MWNTs Composites**

| | Φ (°C/min) | $Z_t$ | $Z_c$ | $n$ |
|---|---|---|---|---|
| Neat PA11 | 2.5 | 0.57 | 0.80 | 2.6 |
| | 5 | 1.95 | 1.14 | 3.0 |
| | 10 | 6.38 | 1.20 | 3.7 |
| | 15 | 12.87 | 1.19 | 3.2 |
| | 20 | 18.05 | 1.16 | 3.2 |
| PA11/MWNTs (0.2%) | 2.5 | 0.03 | 0.25 | 3.2 |
| | 5 | 0.12 | 0.65 | 3.3 |
| | 10 | 0.84 | 0.98 | 3.1 |
| | 15 | 1.84 | 1.04 | 3.1 |
| | 20 | 3.23 | 1.06 | 2.7 |
| PA11/MWNTs (0.5%) | 2.5 | 0.01 | 0.16 | 4.2 |
| | 5 | 0.02 | 0.46 | 5.2 |
| | 10 | 1.38 | 1.03 | 2.7 |
| | 15 | 2.77 | 1.07 | 2.6 |
| | 20 | 4.68 | 1.08 | 2.8 |
| PA11/MWNTs (1.0%) | 2.5 | 0.02 | 0.21 | 3.4 |
| | 5 | 0.06 | 0.57 | 3.8 |
| | 10 | 1.19 | 1.02 | 2.5 |
| | 15 | 2.17 | 1.05 | 2.6 |
| | 20 | 3.52 | 1.06 | 2.8 |

To describe the nonisothermal crystallization process more effectively, a combined model proposed in our previous report was also used here for comparison. The kinetic equation was deduced by combining the Avrami equation with the Ozawa equation and thus a novel equation was obtained as follows[36]:

$$\log Z_t + n \log t = \log K(T) - m \log \Phi \tag{11}$$

which can be further rewritten as follows:

$$\log \Phi = \log F(T) - \alpha \log t \tag{12}$$

where the parameter $F(T) = [K(T)/Z_t]^{1/m}$ refers to the value of cooling rate, which has to be chosen at unit crystallization time when the measured system amounts to a given degree of crystallinity. Figure 8 presents the plots of $\log(\Phi)$ as a function of $\log(t)$. The good linearity of the plots verifies the success of the combined approach applied in this case. The values of $F(T)$ and $\alpha$ at the given relative crystallinity are listed in Table IV. It can be seen that the value of $F(T)$ increases as the relative crystallinity becomes higher, indicating that at unit crystallization time, a higher relative crystallinity can be obtained with a higher cooling rate. In addition, the values of $F(T)$ for PA11/MWNTs nanocomposites were higher than that for neat PA11 at the same $X_t$, suggesting that the addition of MWNTs slowed down the crystal growth process of PA11, which is in agreement with the above results of $t_{1/2}$. For the sample with the same MWNTs loading, the values of $\alpha$ only showed

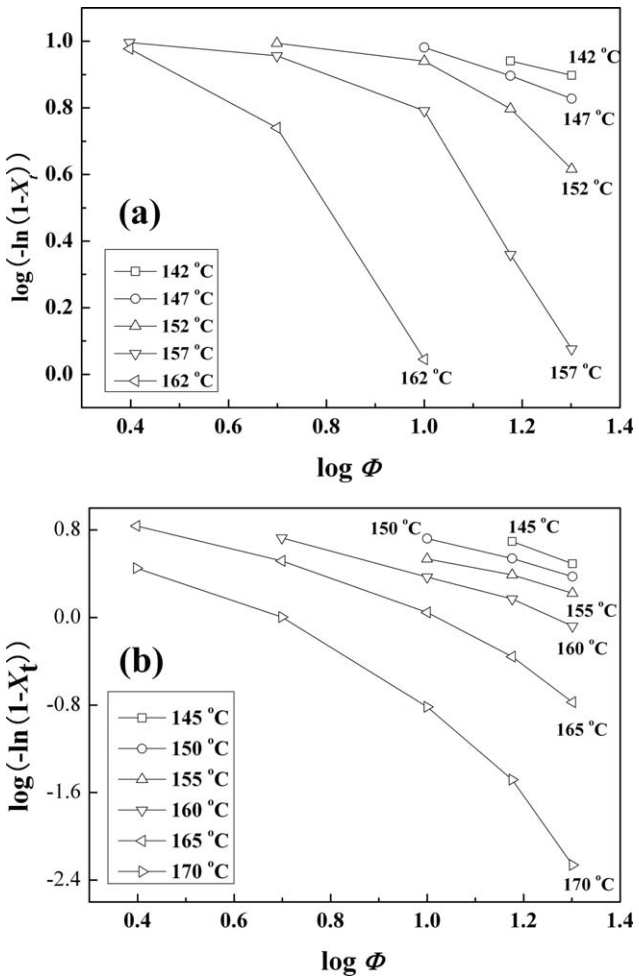


**Figure 7** Ozawa plots of log{−ln[1 − $X(t)$]} versus log(Φ) for nonisothermal melt crystallization of: (a) neat PA11 and (b) PA11/MWNTs (99.8/0.2) nanocomposite.

a slight variation at different relative crystallinities, indicating that the mechanism of nucleation and growth remained the same as the $X_t$ changed. Moreover, the α value of neat PA11 differed obviously from those of the composites with different MWNTs loadings, suggesting that the addition of MWNTs changed the nucleation and growth mechanism of PA11.

Obviously, this combination method can effectively describe the nonisothermal crystallization kinetics of PA11 and its MWNTs composites. The advantage of the combined kinetic model is that it correlates the cooling rate to temperature, time, and morphology (i.e., nucleation and growth mechanism of crystals). Also, this combined method has been proved to be effective in many other polymers and polymer nanocomposites, such as poly(ether ether ketone ketone),[36] poly(ethylene 2,6-naphthalate),[37] poly(3-dodecylthiophene),[38] PA11/ZnO composites,[27] PP/silica nanocomposites,[39] high-density polyethylene/polyhedral oligomer silsesquioxane nanocomposites,[40] PET/antimony-doped tin oxide nanocomposites,[41] PCL/layered double hydroxide nanocomposites,[42] and PA6/MWNTs nanocomposites.[8]

To estimate the effective energy barrier for nonisothermal crystallization process, several mathematic models were proposed to estimate the crystallization activation energy ($\Delta E$) for the transport of polymer chains toward the growing surface. Among them, Kissinger model and Takhor model are the most popular.[43–45] However, Vyazovkin[46] demonstrated that Kissinger model is inappropriate for melt crystallization. Considering the variation of peak temperature ($T_p$) with cooling rate, the activation energy $\Delta E$ could be determined using Takhor model[45]:

$$\frac{d[\ln(\Phi)]}{d(1/T_p)} = -\frac{\Delta E}{R} \tag{13}$$

Figure 9 shows the plots of Takhor model. The crystallization activation energy $\Delta E$ can be calculated from the slopes, i.e., $\Delta E = -R \times$ slope, and the

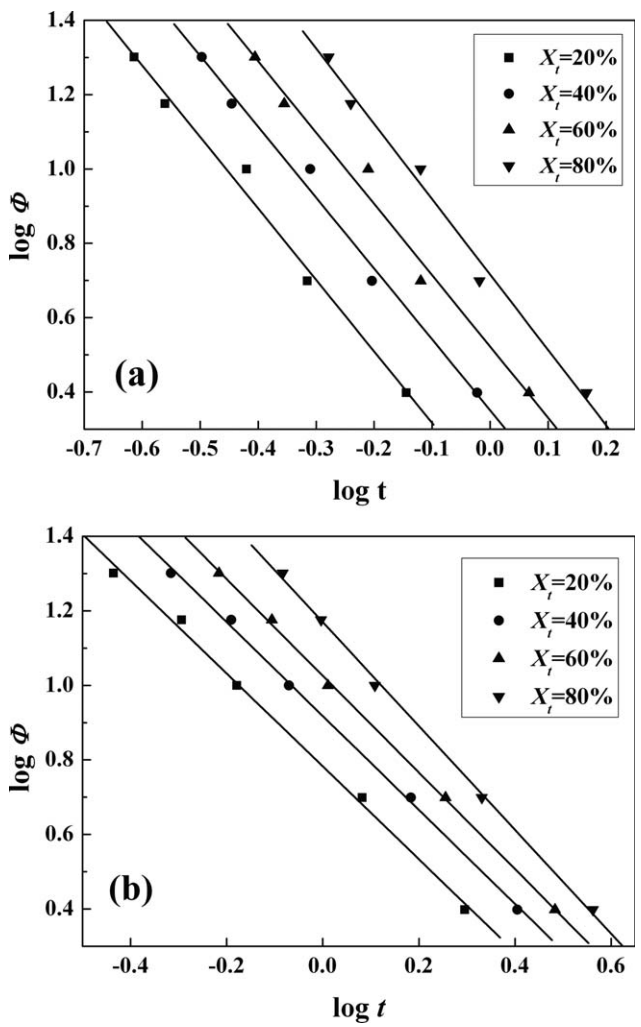


**Figure 8** Plots of log(Φ) versus log($t$) for nonisothermal melt crystallization of (a) neat PA11 and (b) PA11/MWNTs (99.8/0.2) nanocomposite.

**TABLE IV**
**Nonisothermal Melt Crystallization Kinetic Parameters at Different Degrees of Crystallinities by the Combined Avrami–Ozawa Method**

| $X_t$ (%) | | 20 | 40 | 60 | 80 |
|---|---|---|---|---|---|
| Neat PA11 | $F(T)$ | 1.92 | 1.91 | 1.92 | 2.03 |
| | α | 1.33 | 2.24 | 3.33 | 5.2 |
| PA11/MWNTs (0.2%) | $F(T)$ | 1.25 | 1.26 | 1.3 | 1.39 |
| | α | 6.06 | 8.27 | 10.61 | 14.77 |
| PA11/MWNTs (0.5%) | $F(T)$ | 0.98 | 1.03 | 1.07 | 1.12 |
| | α | 5.98 | 7.81 | 9.69 | 12.56 |
| PA11/MWNTs (1.0%) | $F(T)$ | 1.15 | 1.21 | 1.2 | 1.27 |
| | α | 5.75 | 7.77 | 9.86 | 13.16 |

results are listed in Table V. It can be seen that the activation energy of neat PA11 is the lowest, and the value of $\Delta E$ for the composites increases as the loading of MWNTs increases. The crystallization activation energy is closely related to crystallization process and can reveal the potential of crystallization ability. The overall crystallization process usually consists of concurrent nucleation and growth steps. It is well known that polymer chains are highly entangled in the melt and possess relatively high viscosity and low diffusivity. For polymer crystallization, therefore, the chains or chain segments must overcome certain energy barriers to transport (or diffuse) and deposit (or attach) onto the growing front of a crystal. The presence of the MWNTs plays an important role on the nucleation of PA11, and thus the crystallization activation energy of the composites is lower than that of neat PA11. Moreover, the values of crystallization activation energies obtained from nonisothermal crystallization are lower than those from isothermal crystallization. It should be pointed out that the tendency of crystallization activation energy with the MWNTs contents in PA11

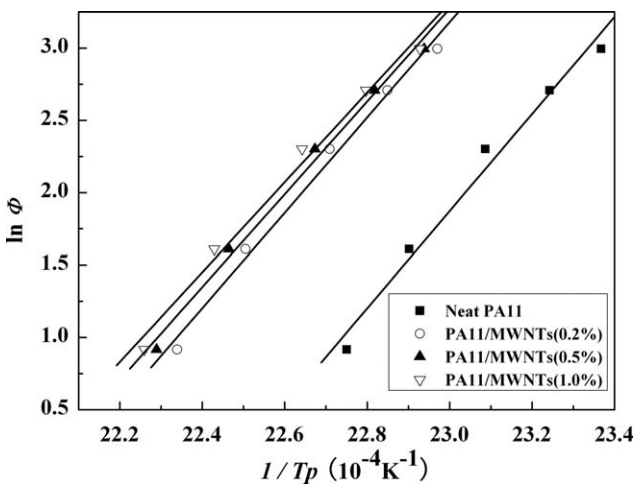


**Figure 9** Plots for estimating the activation energy of nonisothermal melt crystallization of neat PA11 and its composites with different MWNTs contents using Takhor model.

**TABLE V**
**Crystallization Activation Energy $\Delta E$ Calculated from Takhor Model for Nonisothermal Melt Crystallization**

| Samples | $\Delta E$ (kJ/mol) |
|---|---|
| Neat PA11 | 279.2 |
| PA11/MWNTs (0.2%) | 274.0 |
| PA11/MWNTs (0.5%) | 266.5 |
| PA11/MWNTs (1.0%) | 258.0 |

nanocomposites is quite different in both kinetic systems. These results indicate that in nonisothermal crystallization, the nucleation process is the key factor, whereas in isothermal crystallization, the crystal growth process is more dominant. Same conclusion was also made by Wu et al.[6] The results of nonisothermal crystallization activation energy again prove the MWNTs serve as heterogeneous nucleating agent, thus promoting the crystallization process of PA11.

## CONCLUSIONS

A series of PA11 nanocomposites with different MWNTs concentrations has been prepared by melt compounding. The isothermal and nonisothermal melt crystallization kinetics of neat PA11 and its MWNTs composites was comparatively investigated. Avrami equation was used for describing the isothermal crystallization behavior. For the nonisothermal crystallization behavior, the modified Avrami equation, Ozawa method, and the combined Avrami–Ozawa approach were used. During the isothermal crystallization, the MWNTs accelerated crystallization as nucleating agent. The analysis of nonisothermal crystallization process shows that the presence of the MWNTs hinders the mobility of polymer chain and dominates the nonisothermal crystallization process. The activation energy for isothermal and nonisothermal crystallization was estimated. Compared with neat PA11, the activation energy of PA11/MWNTs composites is lower, which is ascribed to the two competitive effects of the MWNTs: acting as nucleation medium to promote crystallization process of PA11 and physical hindrance to retard crystal growth of PA11.

## References

1. Iijima, S. Nature 1991, 354, 56.
2. Baughman, R. H.; Zakhidov, A. A.; de Heer, W. A. Science 2002, 297, 787.
3. Moniruzzaman, M.; Winey, K. I. Macromolecules 2006, 39, 5194.
4. Coleman, J. N.; Khan, U.; Gun'ko, Y. K. Adv Mater 2006, 18, 689.
5. Leelapornpisit, W.; Ton-That, M.-T.; Perrin-Sarazin, F.; Cole, K. C.; Denault, J.; Simard, B. J Polym Sci Part B: Polym Phys 2005, 43, 2445.

6. Wu, T. M.; Chen, E. C. Polym Eng Sci 2006, 46, 1309.
7. Wu, T. M.; Chen, E. C. J Polym Sci Part B: Polym Phys 2006, 44, 498.
8. Li, J.; Fang, Z. P.; Tong, L. F.; Gu, A. J.; Liu, F. Eur Polym Mater 2006, 42, 3230.
9. Li, L. Y.; Li, C. Y.; Ni, C. Y.; Rong, L. X.; Hsiao, B. Polymer 2007, 48, 3452.
10. Shieh, Y. T.; Liu, G. L. J Polym Sci Part B: Polym Phys 2007, 45, 1870.
11. Anand, K. A.; Agarwal, U. S.; Joseph, R. Polymer 2006, 47, 3976.
12. Huang, S.; Wang, M.; Liu, T. X.; Zhang, W. D.; Tjiu, W. C.; He, C. B.; Lu, X. H. Polym Eng Sci 2009, 49, 1063.
13. Zhou, Z. H.; Zeng, H. L.; Gao, C.; Yan, D. Y. Acta Polym Sin 2008, 2, 188.
14. Gunes, I. S.; Cao, F. N.; Jana, S. C. Polymer 2008, 49, 2223.
15. Gunes, I. S.; Jimenez, G. A.; Jana, S. C. Carbon 2009, 47, 981.
16. Gunes, I. S.; Perez-Bolivar, C.; Cao, F. N.; Jimenez, G. A.; Anzenbacher, P.; Jana, S. C. J Mater Chem 2010, 20, 3467.
17. Liu, T. X.; Phang, I. Y.; Shen, L.; Chow, S. Y.; Zhang, W. D. Macromolecules 2004, 37, 7214.
18. Avrami, M. J Chem Phys 1939, 7, 1103.
19. Avrami, M. J Chem Phys 1940, 8, 212.
20. Haggenmueller, R.; Fischer, J. E.; Winey, K. I. Macromolecules 2006, 39, 2964.
21. Kim, K. G.; Newman, B. A.; Scheinbeim, J. I. J Polym Sci Polym Phys Ed 1985, 23, 2477.
22. Deng, H.; Bilotti, E.; Zhang, R.; Wang, K.; Zhang, Q.; Peijs, T.; Fu, Q. J. Appl Polym Sci 2011, 120, 133.
23. Xu, W.; Ge, M.; He, P. J Polym Sci Part B: Polym Phys 2002, 40, 408.
24. Ma, J.; Zhang, S.; Qi, Z.; Li, G.; Hu, Y. J Appl Polym Sci 2002, 83, 1978.
25. Kim, J. Y.; Park, H. S.; Kim, S. H. Polymer 2006, 47, 1379.
26. Ebengou, R. H. J Polym Sci Part B: Polym Phys 1997, 35, 1333.
27. Wu, M.; Yang, G. Z.; Wang, M.; Wang, W. Z.; Zhang, W. D.; Feng, J. C.; Liu, T. X. Mater Chem Phys 2008, 109, 547.
28. Fornes, T. D.; Paul, D. R. Polymer 2003, 44, 3945.
29. Tjong, S. C.; Bao, S. P. J Polym Sci Part B: Polym Phys 2004, 42, 2878.
30. Qiu, Z. B.; Ikehara, T.; Nishi, T. Polymer 2003, 44, 5429.
31. Qiu, Z. B.; Fujinami, S.; Komura, M.; Nakajima, K.; Ikehara, T.; Nishi, T. Polym J 2004, 36, 642.
32. Jeziorny, A. Polymer 1978, 19, 1142.
33. Liu, S. Y.; Yu, Y. N.; Cui, Y.; Zhang, H. F.; Mo, Z. S. J Appl Polym Sci 1998, 70, 2371.
34. Ozawa, T. Polymer 1971, 12, 150.
35. Ozawa, T. J Therm Anal 1976, 9, 369.
36. Liu, T. X.; Mo, Z. S.; Wang, S. E.; Zhang, H. F. Polym Eng Sci 1997, 37, 568.
37. Kim, S. H.; Ahn, S. H.; Hirai, T. Polymer 2003, 44, 5625.
38. Liu, S. L.; Chung, T. S. Polymer 2000, 41, 2781.
39. Jain, S.; Goossens, H.; van Duin, M.; Lemstra, P. Polymer 2005, 46, 8805.
40. Joshi, M.; Butola, B. S. Polymer 2005, 45, 4953.
41. Chen, X. L.; Li, C. Z.; Shao, W.; Liu, T. X.; Wang, L. M. J Appl Polym Sci 2008, 109, 3753.
42. Yang, Z.; Peng, H. D.; Wang, W. Z.; Liu, T. X. J Appl Polym Sci 2010, 116, 2658.
43. Kissinger, H. E. J Res Natl Stand 1956, 57, 217.
44. Kissinger, H. E. J Therm Anal 1957, 9, 369.
45. Takhor, R. L. Advances in Nucleation and Crystallization of Glasses; American Ceramics Society: Columbus, 1971; pp 166–172.
46. Vyazovkin, S. Macromol Rapid Commun 2002, 23, 771.